

# Open-Framework Polar Compounds: Synthesis and Characterization of Rare-Earth Polyoxometalates $(\text{C}_6\text{NO}_2\text{H}_5)_2[\text{Ln}(\text{H}_2\text{O})_5(\text{CrMo}_6\text{H}_6\text{O}_{24})]\cdot 0.5\text{H}_2\text{O}$ ( $\text{Ln} = \text{Ce}$ and $\text{La}$ )

Haiyan An,<sup>[a]</sup> Dongrong Xiao,<sup>[a]</sup> Enbo Wang,<sup>\*,[a]</sup> Yangguang Li,<sup>[a]</sup> Xinlong Wang,<sup>[a]</sup> and Lin Xu<sup>[a]</sup>

**Keywords:** Rare earth / Polyoxometalates / Open framework / Polar compounds / Magnetic properties

Two unprecedented open-framework polar compounds  $(\text{C}_6\text{NO}_2\text{H}_5)_2[\text{Ln}(\text{H}_2\text{O})_5(\text{CrMo}_6\text{H}_6\text{O}_{24})]\cdot 0.5\text{H}_2\text{O}$  [ $\text{Ln} = \text{Ce}$  (**1**),  $\text{La}$  (**2**);  $\text{C}_6\text{NO}_2\text{H}_5$  = pyridine-3-carboxylic acid], constructed from Anderson-type polyoxo anions and rare-earth cations, have been synthesized for the first time and characterized by elemental analysis, IR and Raman spectroscopy, TG analysis, and single-crystal X-ray diffraction. Both compounds crystallize in the polar space group  $Pmn2_1$  and are made up of  $[\text{CrMo}_6\text{H}_6\text{O}_{24}]^{3-}$  polyoxo anions linked by rare-earth cations to form a fascinating 3D open framework with "guest" pyri-

dine-3-carboxylic acid molecules and free water molecules residing in the channels. To the best of our knowledge, this represents the first example of an open-framework polar compound constructed from rare-earth polyoxometalates. The magnetic properties of compound **1** have been studied by measuring its magnetic susceptibility in the temperature range 2.0–300.0 K, indicating the existence of antiferromagnetic interactions.

(© Wiley-VCH Verlag GmbH & Co. KGaA, 69451 Weinheim, Germany, 2005)

## Introduction

Interest in porous polar inorganic materials has increased in recent times, because the potential applications of these materials range from telecommunication, optical storage, and information processing to selective separation and catalysis.<sup>[1]</sup> Although many covalent three-dimensional inorganic frameworks have been reported, few of them possess polarity.<sup>[2]</sup> Thus, the designed construction of porous polar inorganic frameworks is one of the most challenging issues in current synthetic chemistry. While the literature abounds in reports of the synthesis and characterization of aluminosilicates and aluminophosphates with polar and porous architectures,<sup>[3,4]</sup> recently porous polar compounds were extended to systems containing transition-metal oxides because of their particular properties inaccessible in main group systems.<sup>[3]</sup>

Polyoxometalates (POMs),<sup>[7,8]</sup> as anionic early transition metal oxide clusters, have been employed as inorganic building blocks for the construction of larger clusters, or one-, two-, and even three-dimensional (3D) extended solid frameworks, owing to their fascinating properties and potential applications in different areas such as catalysis, mate-

rial science, and biological chemistry. In recent years, several large nanostructured polyoxometalate clusters have been reported by Müller et al.,<sup>[9]</sup> Pope et al.,<sup>[10]</sup> and Yamase et al.,<sup>[11]</sup> a number of 1D and 2D POM-based polymers have also been successfully synthesized by Zubietta et al.<sup>[12]</sup> and Pope et al.<sup>[13]</sup> In contrast, the method of assembling POMs into three-dimensional frameworks, especially open frameworks, is still in its infancy, and has been limited to using the 3d-block elements or their coordination complexes as linkers.<sup>[14,15]</sup> Although rare-earth elements are highly oxophilic and polyoxometalates have oxygen-rich compositions,<sup>[16]</sup> 3D covalent open frameworks containing both of them remain largely unexplored. In addition, special spectroscopic and magnetic properties of lanthanide ions and their compounds have inspired our research interest.<sup>[11,13,17,18]</sup>

Hence, our synthetic strategy starts by finding an appropriate POM building block, and then utilizes rare-earth cations as the linker and organic molecules as the template in an attempt to assemble them into a 3D polar network. More recently, we and others, have prepared a few extended structures based on Anderson-type polyoxo anions, ranging from 1D chains to 2D networks.<sup>[19,20]</sup> The activity of the terminal oxygen atoms on the surface of this kind of POM makes it possible to form 3D covalent structures under an appropriate reaction condition. Furthermore, the employment of low-symmetry organic molecules or complexes as structure-directing agents is promising for the synthesis of new open-framework polar compounds.<sup>[4]</sup> In this experi-

[a] Institute of Polyoxometalate Chemistry, Department of Chemistry, Northeast Normal University, Changchun, 130024, P. R. China  
Fax: +86-431-568-4009

E-mail: wangenbo@public.cc.jl.cn

Supporting information for this article is available on the WWW under <http://www.eurjic.org> or from the author.

ment, we chose the acentric pyridine-3-carboxylic acid molecule as the structure-directing agent instead of the widely utilized organic amines, owing to the requirement for acid reaction conditions. With the pyridine-3-carboxylic acid molecule, we have successfully obtained two unprecedented POM-based compounds possessing polarity and open framework characteristics. Herein, the rational synthesis of the two complexes  $(\text{C}_6\text{NO}_2\text{H}_5)_2[\text{Ln}(\text{H}_2\text{O})_5(\text{CrMo}_6\text{H}_6\text{O}_{24})]\cdot 0.5\text{H}_2\text{O}$  [ $\text{Ln} = \text{Ce}$  (**1**),  $\text{La}$  (**2**)] by this route and magnetic properties of compound **1** are described. It is notable that the 3D polar framework consists of two intersecting channels, within which pyridine-3-carboxylic acid molecules and free water molecules are situated.

## Results and Discussion

The single-crystal X-ray diffraction analyses reveal that both compounds **1** and **2** (Tables 1 and 2) are isostructural and crystallize in the polar space group  $Pmn2_1$ , therefore we only discussed the structure of **1** herein. The structure of **1** is a unique 3D open framework constructed from  $[\text{Cr}(\text{OH})_6\text{Mo}_6\text{O}_{18}]^{3-}$  building blocks and  $\text{Ce}^{3+}$  cations, with pyridine-3-carboxylic acid molecules and lattice water molecules residing in the channels. The  $[\text{Cr}(\text{OH})_6\text{Mo}_6\text{O}_{18}]^{3-}$  cluster is a B-type Anderson structure made up of seven edge-sharing octahedra, six of which are  $\{\text{MoO}_6\}$  octahedra, arranged hexagonally around the central  $\{\text{Cr}(\text{OH})_6\}$  octahedron. Four kinds of oxygen atoms exist in the cluster according to the manner of oxygen coordination: the terminal oxygen atom Ot, the terminal oxygen atom Ot' linked to  $\text{Ce}^{3+}$ , the double-bridging oxygen atom Ob, and the central oxygen atom Oc. Thus, the Mo–O distances can be grouped into four sets: Mo–Ot 1.683(11)–1.732(11) Å, Mo–Ot' 1.727(10)–1.732(9) Å, Mo–Ob 1.909(6)–1.958(9) Å, and Mo–Oc 2.254(7)–2.312(8) Å. The central Cr–Oc distances vary from 1.951(11) to 1.980(11) Å. The bond angles of O–Cr–O range from 83.5(3) to 98.1(3)°.

The asymmetric unit (Figure 1) in the structure of **1** consists of two crystallographically independent one-half Anderson anions, in which both chromium ions [Cr(1) and Cr(2)] occupy special positions, linked by the cerium cation. Crystallographically unique cerium(III), residing in a distorted bicapped square-antiprismatic coordination environment, is defined by four terminal oxygen atoms from four  $[\text{Cr}(\text{OH})_6\text{Mo}_6\text{O}_{18}]^{3-}$  units [average Ce–O 2.491(9) Å] and six water molecules [average Ce–OH<sub>2</sub> 2.626(13) Å]. The average Ce–O bond length is 2.572(11) Å.

In the structure each Anderson anion acts as a quadridentate ligand coordinating to four cerium cations through the terminal oxygen atoms of four  $\{\text{MoO}_6\}$  octahedra. As shown in Figure 2, firstly these  $[\text{Cr}(\text{OH})_6\text{Mo}_6\text{O}_{18}]^{3-}$  clusters are linked by some  $\text{Ce}^{3+}$  cations to form 1D linear chains, then each chain is connected to two other parallel chains through other  $\text{Ce}^{3+}$  cations to yield a window-like 2D layer in the *ac* plane. The 2D layer structure built up of polyoxo anions and rare-earth ions is rare. These 2D sheets are fur-

Table 1. Selected bond lengths [Å] and angles [°] for **1**; symmetry transformations used to generate equivalent atoms: #1:  $-x + 1, -y, -z + 2$ ; #2:  $-x + 2, -y, -z + 1$

Ce(1)–OW4	2.468(19)	Mo(2)–O(11)	1.705(9)
Ce(1)–O(10)#1	2.471(9)	Mo(2)–O(12)	1.732(11)
Ce(1)–O(14)	2.476(9)	Mo(2)–O(6)	1.912(8)
Ce(1)–O(23)	2.502(9)	Mo(2)–O(7)	1.958(9)
Ce(1)–O(28)#2	2.515(9)	Mo(2)–O(2)	2.291(9)
Ce(1)–OW1	2.520(12)	Mo(2)–O(3)	2.301(8)
Ce(1)–OW3	2.523(12)	Mo(3)–O(13)	1.694(10)
Ce(1)–OW2	2.527(13)	Mo(3)–O(14)	1.729(10)
Ce(1)–OW5	2.83(2)	Mo(3)–O(8)	1.909(6)
Ce(1)–OW6	2.888(19)	Mo(3)–O(7)	1.919(8)
Mo(1)–O(9)	1.700(10)	Mo(3)–O(4)	2.254(7)
Mo(1)–O(10)	1.732(9)	Mo(3)–O(3)	2.286(9)
Mo(1)–O(6)	1.916(8)	Cr(1)–O(4)	1.951(11)
Mo(1)–O(5)	1.943(6)	Cr(1)–O(2)	1.960(9)
Mo(1)–O(1)	2.262(7)	Cr(1)–O(1)	1.959(11)
Mo(1)–O(2)	2.301(8)	Cr(1)–O(3)	1.966(8)
O(14)–Ce(1)–O(23)	77.0(3)	OW1–Ce(1)–OW3	75.4(5)
O(14)–Ce(1)–OW3	136.8(4)	OW2–Ce(1)–OW6	58.9(5)
O(14)–Ce(1)–OW5	65.8(5)	OW4–Ce(1)–OW2	139.2(5)
O(14)–Ce(1)–O(28)#2	75.7(3)	OW5–Ce(1)–OW6	175.9(7)
O(14)–Ce(1)–OW1	68.9(4)	O(4)–Cr(1)–O(2)	94.4(3)
O(14)–Ce(1)–OW2	76.7(4)	O(1)–Cr(1)–O(3)	98.1(3)
O(14)–Ce(1)–OW6	118.3(5)	O(9)–Mo(1)–O(10)	106.6(5)
O(23)–Ce(1)–OW3	145.7(4)	O(6)–Mo(1)–O(1)	82.9(3)
O(23)–Ce(1)–OW2	69.3(3)	O(5)–Mo(1)–O(2)	84.0(4)
O(23)–Ce(1)–OW6	117.4(4)	O(11)–Mo(2)–O(12)	106.2(5)
O(10)#1–Ce(1)–OW6	65.8(5)	O(6)–Mo(2)–O(7)	148.1(3)
O(10)#1–Ce(1)–O(23)	71.3(3)	O(2)–Mo(2)–O(3)	70.1(3)
OW1–Ce(1)–OW6	60.3(5)	O(13)–Mo(3)–O(14)	104.9(5)
OW1–Ce(1)–OW2	75.0(4)	O(8)–Mo(3)–O(7)	149.6(4)
OW1–Ce(1)–OW5	122.5(5)	O(4)–Mo(3)–O(3)	70.1(3)

ther pillared by the  $[\text{Cr}(\text{OH})_6\text{Mo}_6\text{O}_{18}]^{3-}$  subunits to form a 3D open framework. It is notable that this kind of connection mode results in the formation of two intersecting channels, which are occupied by the dissociated pyridine-3-carboxylic acid molecules (see Figure 3) and lattice water molecules. The dimensions of the two channels are about  $10.0 \times 8.5$  Å along the *a* axis (shown in Figure 4) and  $10.7 \times 6.2$  Å along the *b* axis, respectively (see Figure 5). It is also striking that the structure of compound **1** exhibits extensive hydrogen-bonding interactions among water molecules, pyridine-3-carboxylic acid molecules, and polyoxo anions. The typical hydrogen bonds are O37...O2 2.784, O36...O16 2.641, O37...OW3 2.922, O9...C5 3.119, and O6...C23 2.682 Å (shown in Table S1). It is believed that the extensive hydrogen-bonding interactions between guest molecules and the framework play an important role in stabilizing the 3D structure. Worth mentioning here is that the observed polarity of **1**, indicated by its polar space group  $Pmn2_1$ , can be partially understood in terms of the molecular recognition between the host framework and guest molecule template through hydrogen bonds.<sup>[21,22]</sup>

The bond valence sum calculations indicate that the Cr site is in the +3 oxidation state, Ce and La sites are in the +3 oxidation state, and all Mo sites are in the +6 oxidation state.<sup>[23]</sup>

Table 2. Selected bond lengths [ $\text{\AA}$ ] and angles [ $^\circ$ ] for **2**; symmetry transformations used to generate equivalent atoms: #1:  $-x + 1/2, -y + 3, z - 1/2$ ; #2:  $x, y + 1, z$

La(1)–O(23)#1	2.470(12)	Mo(1)–O(10)	1.715(12)
La(1)–OW4	2.47(2)	Mo(1)–O(5)	1.919(8)
La(1)–O(28)	2.488(12)	Mo(1)–O(6)	1.932(10)
La(1)–OW1	2.531(15)	Mo(1)–O(1)	2.281(9)
La(1)–O(14)	2.530(11)	Mo(1)–O(2)	2.335(11)
La(1)–O(10)#2	2.535(11)	Mo(2)–O(12)	1.667(12)
La(1)–OW3	2.581(14)	Mo(2)–O(11)	1.705(12)
La(1)–OW2	2.622(15)	Mo(2)–O(7)	1.936(12)
La(1)–OW5	2.85(2)	Mo(2)–O(6)	1.945(12)
La(1)–OW6	2.90(3)	Mo(2)–O(2)	2.256(11)
Mo(1)–O(9)	1.689(15)	Mo(2)–O(3)	2.309(11)
Mo(3)–O(13)	1.701(13)	Cr(1)–O(3)	1.961(10)
Mo(3)–O(3)	2.277(12)	Cr(1)–O(1)	1.978(15)
Mo(3)–O(7)	1.906(10)	Cr(1)–O(4)	1.979(15)
Mo(3)–O(8)	1.932(7)	Cr(1)–O(2)	1.978(10)
O(23)#1–La(1)–O(28)	143.8(4)	OW2–La(1)–OW6	57.2(7)
O(23)#1–La(1)–O(10)#2	76.8(4)	OW1–La(1)–OW3	74.5(5)
O(23)#1–La(1)–OW3	76.3(5)	O(9)–Mo(1)–O(10)	105.8(7)
O(23)#1–La(1)–OW2	137.8(5)	O(5)–Mo(1)–O(6)	150.9(6)
O(23)#1–La(1)–OW6	119.0(8)	O(1)–Mo(1)–O(2)	71.4(4)
O(23)#1–La(1)–OW4	119.6(7)	O(11)–Mo(2)–O(6)	99.4(6)
O(23)#1–La(1)–OW5	64.0(7)	O(7)–Mo(2)–O(2)	83.2(4)
O(14)–La(1)–OW3	142.5(5)	O(12)–Mo(2)–O(3)	93.4(5)
O(14)–La(1)–O(10)#2	125.7(4)	O(13)–Mo(3)–O(7)	98.9(6)
O(14)–La(1)–OW5	62.1(5)	O(14)–Mo(3)–O(7)	102.5(5)
O(14)–La(1)–OW6	116.6(6)	O(14)–Mo(3)–O(4)	158.3(6)
OW3–La(1)–OW6	59.4(6)	O(3)–Cr(1)–O(1)	95.8(5)
O(28)–La(1)–OW5	112.7(7)	O(4)–Cr(1)–O(2)	94.8(4)

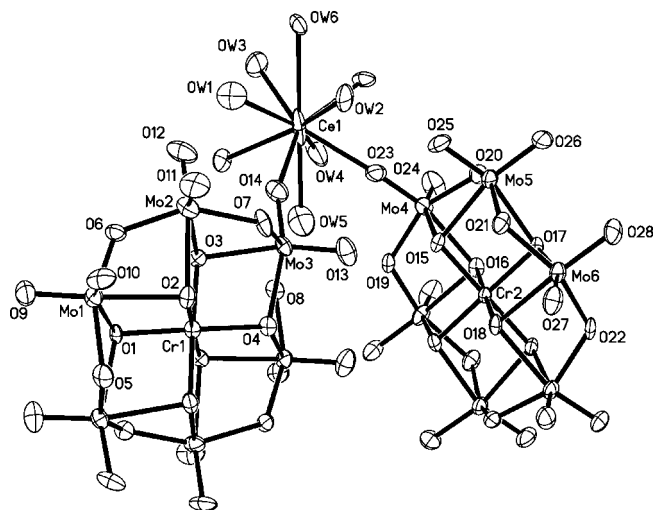


Figure 1. ORTEP drawing of compound **1** with thermal ellipsoids at 50% probability; organic molecules and partial water molecules are omitted for clarity

In the IR spectrum of compound **1**, the features at 3368, 2094, 1635, 1558, 1401, 1374, 1357, and 1304  $\text{cm}^{-1}$  can be regarded as characteristic of the pyridine-3-carboxylic acid molecule. The peaks at 946, 909, 879, 759, 649, 578, and 412  $\text{cm}^{-1}$  are attributed to  $\nu(\text{Mo}-\text{Ot})$ ,  $\nu(\text{Mo}-\text{Ob})$ , and  $\nu(\text{Mo}-\text{Oc})$  of the  $[\text{Cr}(\text{OH})_6\text{Mo}_6\text{O}_{18}]^{3-}$  polyoxo anion. The IR spectrum of compound **2** is similar to that of **1** (see Figures S3a and S3b in the Supporting information). In the

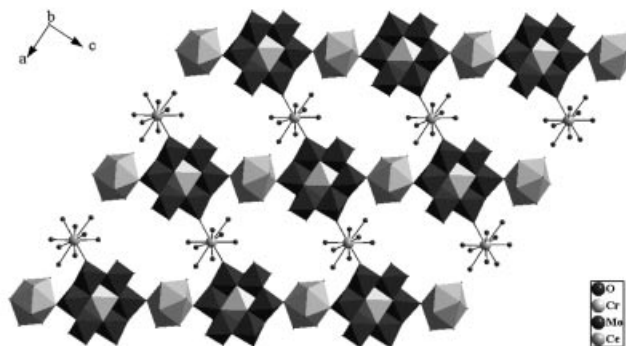


Figure 2. Polyhedral view of the 2D network in **1**

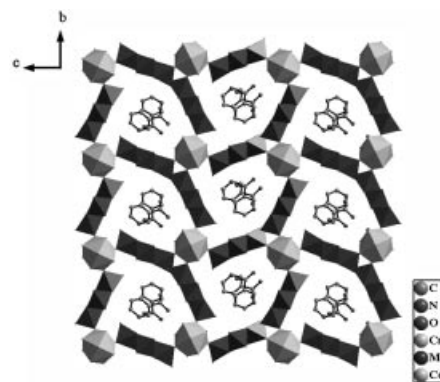


Figure 3. Polyhedral view of the 3D open framework of **1** viewing along the *a* axis, containing pyridine-3-carboxylic acid molecules in the channels

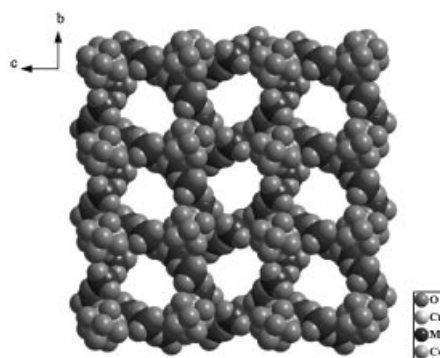


Figure 4. Space-filling diagram of the 3D open framework of **1** along the *a* axis, showing the 1D channels

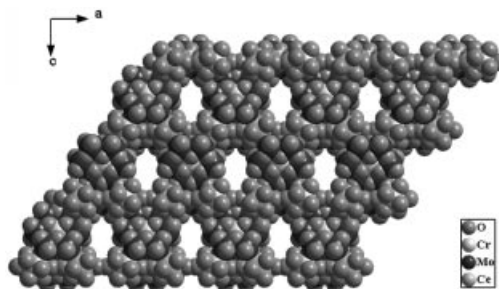


Figure 5. Space-filling diagram of the 3D porous structure of **1** along the *b* axis, representing the 1D channels



Raman spectrum of compound **1**, the bands at 993, 942, 821, 713, 449, 337, and 286  $\text{cm}^{-1}$  are ascribed to the  $[\text{Cr}(\text{OH})_6\text{Mo}_6\text{O}_{18}]^{3-}$  polyoxo anion. In the Raman spectrum of compound **2**, the features at 993, 929, 908, 850, 823, 550, 333, and 250  $\text{cm}^{-1}$  are also attributed to the  $[\text{Cr}(\text{OH})_6\text{Mo}_6\text{O}_{18}]^{3-}$  polyoxo anion (shown in Figure S4).

The thermal gravimetric (TG) curve of **1** is shown in Figure S5a. The TG curve gives a total weight loss of 27.24% in the range of 45–750  $^{\circ}\text{C}$ , which agrees with the calculated value of 26.55%. The weight loss of 10.60% at 45–300  $^{\circ}\text{C}$  corresponds to the loss of all noncoordinated and coordinated water molecules (calcd. 10.18%). The weight loss of 16.64% at 340–575  $^{\circ}\text{C}$  arises from the decomposition of organic molecules (calcd. 16.37%). The TG curve of compound **2** exhibits similar weight loss stages to those of compound **1** (see Figure S5b). The whole weight loss (27.16%) is in agreement with the calculated value (26.57%).

### Magnetic Properties of Compound 1

The structure of  $[\text{Cr}(\text{OH})_6\text{Mo}_6\text{O}_{18}]^{3-}$  clusters bridged by  $\text{Ce}^{3+}$  cations in compound **1** allows us to predict the existence of magnetic exchange coupling. The thermal variations of  $\chi_{\text{M}}T$  and  $1/\chi$  of **1** are displayed in Figure 6. The value of  $\chi_{\text{M}}T$  continuously decreases as the temperature is lowered from 300.0 to 2.0 K, indicating the presence of an antiferromagnetic interaction. At 300 K, the  $\chi_{\text{M}}T$  value is ca. 2.87  $\text{emu K mol}^{-1}$  ( $4.79 \mu_{\text{B}}$ ), slightly higher than the total value (2.25  $\text{emu K mol}^{-1}$ ,  $4.24 \mu_{\text{B}}$ ) of one uncoupled  $S = 3/2$  spin of the  $\text{Cr}^{3+}$  atom and one uncoupled  $S = 1/2$  spin of the  $\text{Ce}^{3+}$  atom. The magnetic susceptibility obeys the Curie–Weiss law in the whole range of 2.0–300.0 K with  $C = 2.81 \text{ emu K mol}^{-1}$ , and  $\theta = -5.79 \text{ K}$ , characteristic of an overall antiferromagnetic interaction. It is too difficult to fit the experimental magnetic data of this complex system using a suitable theoretical model, and further studies on magnetic properties of similar systems are ongoing in our laboratory.

### Conclusions

In conclusion, we have synthesized the only structurally characterized rare-earth POM complexes featuring an open framework and polarity reported until now, by choosing a suitable POM building block, organic template, and suitable reaction conditions. The success in synthesizing both compounds provides not only innovative examples of open-framework polar compounds, but also a new strategy for the design of polar inorganic materials with channels based on POMs. In contrast to the famous aluminosilicates and metal phosphates with porous polar frameworks, this new type of POM-based polar compound represents another important branch in the field of polarity and open-framework perspectives in the study of these materials. The magnetic properties of **1** have been studied and its antiferromagnetic behavior results from the transformation of O–Mo–O units.

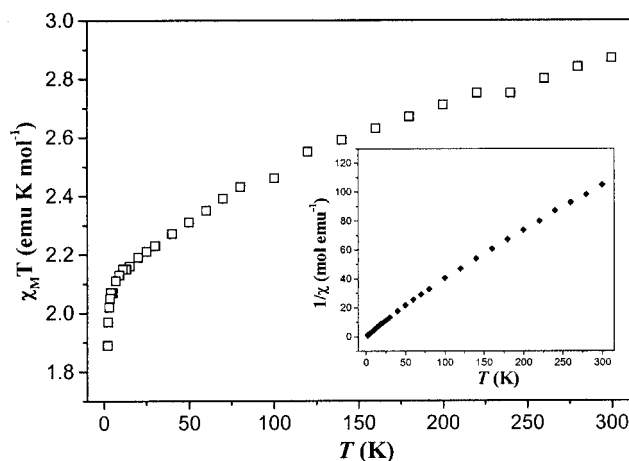


Figure 6. The temperature dependence of reciprocal magnetic susceptibility  $\chi_{\text{M}}^{-1}$  (diamonds; inset) and the product  $\chi_{\text{M}}T$  (squares) for compound **1**

### Experimental Section

**Materials and General Methods:** All chemicals were commercially purchased and used without further purification.  $\text{Na}_3[\text{CrMo}_6\text{H}_6\text{O}_{24}]\cdot 8\text{H}_2\text{O}$  was synthesized according to the literature,<sup>[24]</sup> and characterized by IR spectra and TG analyses. Elemental analyses (C, H, and N) were performed with a Perkin–Elmer 2400 CHN elemental analyzer; Cr, Mo, Ce, and La were analyzed with a PLASMA-SPEC(I) ICP atomic emission spectrometer. IR spectra were recorded in the range 400–4000  $\text{cm}^{-1}$  with an Alpha Centaur FT/IR spectrophotometer using KBr pellets. TG analyses were performed with a Perkin–Elmer TGA7 instrument in flowing  $\text{N}_2$  with a heating rate of 10  $^{\circ}\text{C min}^{-1}$ . The Raman spectrum was recorded at ambient temperature with a Spex 1403 Raman spectrometer with an argon ion laser at an excitation wavelength of 514.5 nm. Variable-temperature magnetic susceptibility data were obtained with a SQUID magnetometer (Quantum Design, MPMS-7) in the temperature range of 2.0–300.0 K with an applied field of 10 kG.

**Synthesis of 1:** In a typical synthesis procedure for **1**, first pyridine-3-carboxylic acid (0.0616 g, 0.5 mmol) and then  $\text{Ce}(\text{NO}_3)_3\cdot 6\text{H}_2\text{O}$  (0.2171 g, 0.5 mmol) were dissolved in hot water (10 mL). Then an aqueous solution (10 mL) of  $\text{Na}_3[\text{CrMo}_6\text{H}_6\text{O}_{24}]\cdot 8\text{H}_2\text{O}$  (0.6155 g, 0.5 mmol) was added to the above solution. The initial pH value of this mixture was 3.00. The mixture was then refluxed at 80  $^{\circ}\text{C}$  for 1 h. The filtrate was kept under ambient conditions for 2 weeks, then yellow block crystals of compound **1** were isolated in about 45% yield (0.338 g, based on Ce).  $\text{C}_{12}\text{H}_{27}\text{CeCrMo}_6\text{N}_2\text{O}_{33.50}$ : calcd. C 9.58, Ce 9.32, Cr 3.46, Mo 38.30, N 1.86; found C 9.33, Ce 9.50, Cr 3.23, Mo 36.61, N 1.95. FT IR:  $\tilde{\nu} = 3368$  (s), 2094 (w), 1635 (m), 1558 (m), 1461 (w), 1401 (m), 1374 (m), 1357 (m), 1304 (w), 1109 (w), 946 (s), 909 (vs), 879 (s), 838 (w), 759 (m), 690 (w), 649 (vs), 618 (w), 578 (w), 541 (w), 412 (m)  $\text{cm}^{-1}$ .

**Synthesis of 2:** The preparation of **2** was similar to that of **1** except that  $\text{La}(\text{NO}_3)_3\cdot 6\text{H}_2\text{O}$  was used instead of  $\text{Ce}(\text{NO}_3)_3\cdot 6\text{H}_2\text{O}$  (0.375 g, yield 50%).  $\text{C}_{12}\text{H}_{27}\text{CrLaMo}_6\text{N}_2\text{O}_{33.50}$ : calcd. C 9.59, Cr 3.46, La 9.25, Mo 38.33, N 1.86; found C 9.71, Cr 3.20, La 9.62, Mo 36.55, N 1.68. FT IR:  $\tilde{\nu} = 3367$  (s), 1633 (m), 1563 (m), 1464 (w), 1393 (m), 1303 (w), 1182 (w), 1108 (w), 946 (s), 909 (vs), 887 (s), 838 (w), 760 (m), 649 (vs), 581 (w), 411 (m)  $\text{cm}^{-1}$ .

Table 3. Crystal data and structure refinement for **1** and **2**

Complex	<b>1</b>	<b>2</b>
Empirical formula	C <sub>12</sub> H <sub>27</sub> CeCrMo <sub>6</sub> N <sub>2</sub> O <sub>33.50</sub>	C <sub>12</sub> H <sub>27</sub> LaCrMo <sub>6</sub> N <sub>2</sub> O <sub>33.50</sub>
Formula mass	1503.12	1501.91
<i>T</i> [K]	293(2)	293(2)
$\lambda$ [Å]	0.71073	0.71073
Space group	<i>Pmn</i> 2 <sub>1</sub>	<i>Pmn</i> 2 <sub>1</sub>
<i>a</i> [Å]	15.0314(9)	15.080(3)
<i>b</i> [Å]	11.6090(7)	11.630(2)
<i>c</i> [Å]	23.0481(14)	23.096(5)
<i>V</i> [Å <sup>3</sup> ]	4021.9(4)	4050.6(14)
<i>Z</i>	4	4
<i>D</i> <sub>calcd.</sub> [g cm <sup>-3</sup> ]	2.482	2.463
$\mu$ [mm <sup>-1</sup> ]	3.278	3.186
<i>R</i> <sub>1</sub> <sup>[a]</sup> [ <i>I</i> > 2σ( <i>I</i> )]	0.0511	0.0637
<i>wR</i> <sub>2</sub> <sup>[b]</sup> [ <i>I</i> > 2σ( <i>I</i> )]	0.1360	0.1535

[a]  $R_1 = \sum \|F_o| - |F_c| \| / \sum |F_o|$ . [b]  $wR_2 = \sum [w(F_o^2 - F_c^2)^2] / \sum [w(F_o^2)^2]^{1/2}$ .

**X-ray Crystallography:** Suitable single crystals with dimensions of  $0.26 \times 0.13 \times 0.05$  mm for **1** and  $0.32 \times 0.28 \times 0.03$  mm for **2** were selected for single-crystal X-ray diffraction analysis. Data were collected with a Bruker Smart Apex CCD diffractometer with Mo-*K*<sub>α</sub> ( $\lambda = 0.71073$  Å) at 293 K using the  $\omega$ -scan technique. Empirical absorption correction was applied. Systematic absences and the statistics of intensity distribution resulted in the space group *Pmn*2<sub>1</sub>. The structures of **1** and **2** were solved by the direct method and refined by the full-matrix least squares on *F*<sup>2</sup> using the SHELXTL-97 software.<sup>[25]</sup> All of the non-hydrogen atoms were refined anisotropically except for C22 and O37 in **1** and O4, O18, O19, and O36 in **2**. In **1**, positions of the hydrogen atoms attached to polyanions and to coordinated water molecules except for OW4 were located from difference maps, and those attached to carbon atoms were fixed in ideal positions; the hydrogen atoms attached to OW4, free OW7, and to oxygen atoms of carboxyl groups were not located. In **2**, positions of the hydrogen atoms attached to carbon atoms were fixed in ideal positions and other hydrogen atoms are not located. A summary of the crystallographic data and structural determination for **1** and **2** is provided in Table 3. Selected bond lengths and angles of **1** and **2** are listed in Tables 1 and 2, respectively. CCDC-245443 and -245641 contain the supplementary crystallographic data for this paper. These data can be obtained free of charge from The Cambridge Crystallographic Data Centre via [www.ccdc.cam.ac.uk/data\\_request/cif](http://www.ccdc.cam.ac.uk/data_request/cif).

## Acknowledgments

The authors thank the National Natural Science Foundation of China (20371011) for financial support.

- [1] M. E. Davis, *Nature* **2002**, 417, 813–821.
- [2] a) M. L. Tong, S. L. Zheng, X. M. Chen, *Chem. Commun.* **1999**, 561–562; b) J. Tao, M. L. Tong, X. M. Chen, *J. Chem. Soc., Dalton Trans.* **2000**, 20, 3669–3674; c) X. L. Wang, C. Qin, E. B. Wang, Y. G. Li, C. W. Hu, L. Xu, *Chem. Commun.* **2004**, 378–379.
- [3] a) M. E. Davis, *Acc. Chem. Res.* **1993**, 26, 111–115; b) M. M. J. Treacy, J. M. Newsam, *Nature* **1988**, 332, 249–251.
- [4] a) K. Morgan, G. Gainsford, N. Milestone, *Chem. Commun.* **1995**, 425–426; b) W. T. A. Harrison, T. E. Gier, G. D. Stucky, R. W. Broach, R. A. Bedard, *Chem. Mater.* **1996**, 8, 145–151; c) D. A. Bruce, A. P. Wilkinson, M. G. White, J. A. Bertrand, *Chem. Commun.* **1995**, 2059–2060.
- [5] a) N. Ding, D. Y. Chung, M. G. Kanatzidis, *Chem. Commun.* **2004**, 1170–1171; b) T. A. Sullens, R. A. Jensen, T. Y. Shvareva, T. E. Albrecht-Schmitt, *J. Am. Chem. Soc.* **2004**, 126, 2676–2677; c) Y. Wang, J. H. Yu, M. Guo, R. R. Xu, *Angew. Chem. Int. Ed.* **2003**, 42, 4089–4092.
- [6] H. S. Ra, K. M. Ok, P. S. Halasyamani, *J. Am. Chem. Soc.* **2003**, 125, 7764–7765.
- [7] a) M. T. Pope, *Heteropoly and Isopoly Oxometalates*, Springer, Berlin, **1983**; b) C. L. Hill, *Chem. Rev.* **1998**, 98, 1–2.
- [8] a) U. Kortz, S. S. Hamzeh, N. A. Nasser, *Chem. Eur. J.* **2003**, 9, 2945–2952; b) U. Kortz, M. G. Savelieff, B. S. Bassil, B. Keita, L. Nadjo, *Inorg. Chem.* **2002**, 41, 783–789; c) E. Coronado, J. R. Galán-Mascarós, C. Giménez-Saiz, C. J. Gómez-García, S. Triki, *J. Am. Chem. Soc.* **1998**, 120, 4671–4681.
- [9] a) A. Müller, S. Q. N. Shah, H. Bögge, M. Schmidtman, *Nature* **1999**, 397, 48–50; b) L. Cronin, C. Beugholt, E. Krickemeyer, M. Schmidtman, H. Bögge, P. Kögerler, T. K. K. Luong, A. Müller, *Angew. Chem. Int. Ed.* **2002**, 41, 2805–2808.
- [10] K. Wassermann, M. H. Dickman, M. T. Pope, *Angew. Chem. Int. Ed. Engl.* **1997**, 36, 1445–1448.
- [11] K. Fukaya, T. Yamase, *Angew. Chem. Int. Ed.* **2003**, 42, 654–658.
- [12] P. J. Hagrman, D. Hagrman, J. Zubieta, *Angew. Chem. Int. Ed.* **1999**, 38, 3165–3168.
- [13] a) M. Sadakane, M. H. Dickman, M. T. Pope, *Angew. Chem. Int. Ed.* **2000**, 39, 2914–2916; b) K. C. Kin, M. T. Pope, *J. Am. Chem. Soc.* **1999**, 121, 8512–8517.
- [14] a) M. I. Khan, E. Yohannes, D. Powell, *Chem. Commun.* **1999**, 23–24; b) M. I. Khan, E. Yohannes, R. J. Doedens, *Angew. Chem. Int. Ed.* **1999**, 38, 1292–1294.
- [15] a) B. Z. Lin, S. X. Liu, *Chem. Commun.* **2002**, 2126–2127; b) Y. G. Li, N. Hao, E. B. Wang, M. Yuan, C. W. Hu, N. H. Hu, H. Q. Jia, *Inorg. Chem.* **2003**, 42, 2729–2735; c) M. Yuan, Y. G. Li, E. B. Wang, Y. Lu, C. W. Hu, N. H. Hu, H. Q. Jia, *J. Chem. Soc., Dalton Trans.* **2002**, 2916–2920.
- [16] a) R. C. Howell, F. G. Perez, S. Jain, W. D. Horrocks, A. L. Rheingold, L. C. Francesconi, *Angew. Chem. Int. Ed.* **2001**, 40, 4031–4033; b) C. D. Wu, C. Z. Lu, H. H. Zhuang, J. S. Huang, *J. Am. Chem. Soc.* **2002**, 124, 3836–3837; c) M. R. Antonio, L. Soderholm, C. W. Williams, N. Ullah, L. C. Francesconi, *J. Chem. Soc., Dalton Trans.* **1999**, 3825–3830.
- [17] X. L. Wang, Y. Q. Guo, Y. G. Li, E. B. Wang, C. W. Hu, N. H. Hu, *Inorg. Chem.* **2003**, 42, 4135–4140.
- [18] a) A. Dolbecq, P. Mialane, L. Lisnard, J. Marrot, F. Sécheresse, *Chem. Eur. J.* **2003**, 9, 2914–2920; b) J. Y. Niu, M. L. Wei, J. P. Wang, D. B. Dang, *Eur. J. Inorg. Chem.* **2004**, 160–170.
- [19] a) H. Y. An, Y. Lan, Y. G. Li, E. B. Wang, N. Hao, D. R. Xiao, L. Y. Duan, L. Xu, *Inorg. Chem. Commun.* **2004**, 7, 356–358;

- b) H. Y. An, Y. Q. Guo, Y. G. Li, E. B. Wang, J. Lü, L. Xu, C. W. Hu, *Inorg. Chem. Commun.* **2004**, 7, 521–523.
- [20] a) V. Shivaiah, P. V. N. Reddy, L. Cronin, S. K. Das, *J. Chem. Soc., Dalton Trans.* **2002**, 3781–3783; b) D. Drewes, E. M. Limanski, B. Krebs, *J. Chem. Soc., Dalton Trans.* **2004**, 2087–2091.
- [21] S. P. D. Huang, R. G. Xiong, *Polyhedron* **1997**, 16, 3929–3939.
- [22] S. P. Anthony, T. P. Radhakrishnan, *Chem. Commun.* **2001**, 931–932.
- [23] I. D. Brown, D. Altermatt, *Acta Crystallogr., Sect. B* **1985**, 41, 244.
- [24] A. Perloff, *Inorg. Chem.* **1970**, 9, 2228–2239.
- [25] a) G. M. Sheldrick, *SHELXL-97, Program for Crystal Structure Refinement*, University of Göttingen, Germany, **1997**; b) G. M. Sheldrick, *SHELXL-97, Program for Crystal Structure Solution*, University of Göttingen, Germany, **1997**.

Received: August 13, 2004